

## On the micromechanisms of fatigue long crack growth under remote shear loading modes

Libor Holáň<sup>1, a</sup>, Anton Hohenwarter<sup>2, b</sup>, Karel Slámečka<sup>1, c</sup>, Reinhard Pippan<sup>2, d</sup>  
and Jaroslav Pokluda<sup>1, e</sup>

<sup>1</sup>Brno University of Technology, Faculty of Mechanical Engineering, Technická 2, 616 69 Brno, Czech Republic

<sup>2</sup>Erich Schmid Institute of Materials Science, Austrian Academy of Sciences, Jahnstrasse 12, 8700 Leoben, Austria

<sup>a</sup>y101840@stud.fme.vutbr.cz, <sup>b</sup>anton.hohenwarter@unileoben.ac.at, <sup>c</sup>slamecka@vutbr.cz, <sup>d</sup>pippan@unileoben.ac.at, <sup>e</sup>pokluda@fme.vutbr.cz

**Keywords:** fatigue, shear mode, crack propagation, quantitative fractography

**Abstract.** An original experimental setup allowing simultaneous mode I and mode II crack propagation in a single specimen is described in detail and some of the first achieved results are presented. The differences between the long fatigue crack propagation under both modes are assessed by means of the fractographical analysis in circumferentially notched cylindrical specimens made of austenitic steel. It is concluded that, based on the 3D observation and the roughness analysis, the crack propagation mechanism is distinctively different within remote modes II and III regions.

### Introduction

So far, the experiments allowing simultaneous mode II and mode III crack propagation in a single specimen were performed only in a pure torsion. Nevertheless, this case of loading creates hardly very difficult solvable problems. Therefore, the original testing setup enabling pure shear loading of specimen has been designed.

Model of Pokluda and Pippan [1] explains the micromechanisms of cracks propagation in ductile metals under shear mode III as an alternating step-by-step growth of the crack front segments in a pure mode II mechanism (Fig.1). This model assumes, that the crack front is never microscopical straight, therefore the microscopical mode II is always present in microscopic pure mode III.

However, while the principal micromechanisms of fatigue crack growth under modes I and II are well known, there is a lack of any plausible interpretation in case of a pure mode III crack propagation. The main reason lies in the fact that, when a pure mode III is present, new segments of fracture surface are generated by screw dislocations aside the crack front, i.e. perpendicularly to the crack propagation direction. On the other hand, the crack incremental advance along the whole front is generated by edge dislocations in modes I and II. Although mode III lateral “ledges” might propagate as local mode II segments it is clearly perceived that the overall crack growth rate should be much lower than the straightforward crack growth under modes I and II.

The first experiments in pure shear loading were performed in work Pokluda et. al. [2], where the specimens were loaded by cyclic shear loading in low cycle fatigue. The authors assume that the present observations do not indicate a pure mode III crack extension. In ductile materials, the crack propagation under mode III fatigue loading is locally by mixed mode I and II mechanisms. The fractographical observations confirmed that the crack front under remote mode III is more spatially tortuous and branched than that under remote mode II. Observed morphological features confirm that, similarly to the remote mode II loading, both pure mode II and combined mode I + II are dominating microscopical fracture mechanisms also during the remote mode III loading.

The aim of the paper is to present a description of the prototype experiment that allows simultaneous mode II and mode III crack propagation in a single specimen in high cycle fatigue.

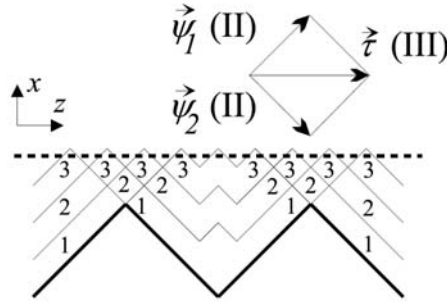


Fig. 1, Scheme of the alternating pure mode II mechanism leading to a gradual advance of a microscopically tortuous (macroscopically straight) crack front, in a macroscopic mode III. The thin lines indicate positions of the crack front after specific fatigue cycles [1].

**Experimental procedure**

For the purpose of the experimental verification of the fatigue long crack behaviour under modes II and III the original testing setup has been designed and utilized in cooperation with Erich Schmid Institute of Materials Science, Austrian Academy of Sciences, in Leoben. In order to assure both pure remote shear modes II and III crack propagation in a single specimen, a special loading cell was manufactured, Fig. 2. As shown in Fig. 3 a, b, the construction of the specimen holder and its orientation in respect to the loading axis provide a pure Mode II operation at the “top” and “bottom” specimen sites and a pure Mode III at “front” and “back” sites.

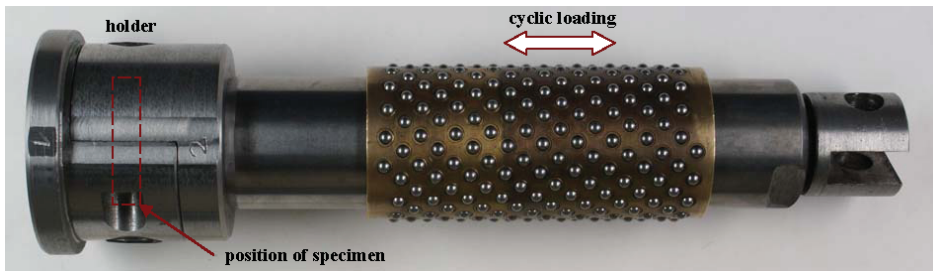


Fig. 2, A photograph of the loading cell. The position of the specimen in a holder and the loading direction are indicated.

Two cylindrical specimen were made of the X2CrNiMo18-14-3 austenitic steel grade with yield strength  $\sigma_y = 200$  MPa. Circumferential V-notch was machined by a lathe tool at a specimen mid-length in which a sharp pre-crack was introduced by a blade mechanism, see Fig. 4. Constant pressure on the gripping frame transferring onto the blade and the specimen undergoing both the rotational and translational motions during procedure guarantee the symmetry and sharpness of the initial pre-crack. Note that although special care was taken during both the notch machining operation and the pre-cracking procedure, the front of the pre-crack could not be considered to be microscopically perfectly smooth. Therefore, the cyclic shear plasticity at the notch-root should be high enough to overlay initial microroughness and to produce a rather homogeneous process zone around the notch.

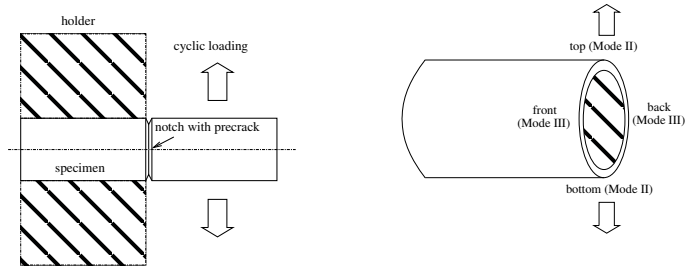


Fig. 3, (a) The loading scheme, (b) the loading modes operating at different specimen sites

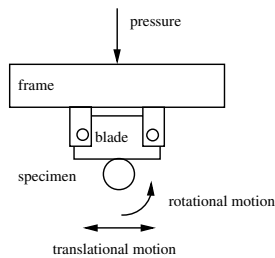


Fig. 4, Sketch of the pre-cracking procedure

Specimens were tested using shear loading of the amplitude  $\tau_a = 180$  MPa and the loading ratio  $R = \tau_{\min} / \tau_{\max} = 0.1$  as the loading regime, where  $\tau_{\min}$  and  $\tau_{\max}$  are minimal and maximal loading levels. Both experiments were interrupted after 380 000 cycles and cyclic tensile loading of the amplitude  $\sigma_a = 200$  MPa and the loading ratio  $R = 0.1$  was applied afterwards until a final fracture occurred, Fig. 5 and Fig. 6.

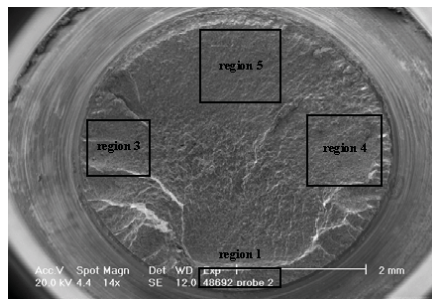


Fig. 5, Fracture surface of tested specimen. Rectangular regions chosen for the fractographical analysis are specified and numbered. The remote mode II acts on the crack front located within the regions 1 and 5, while the remote mode III is present within regions 3 and 4.

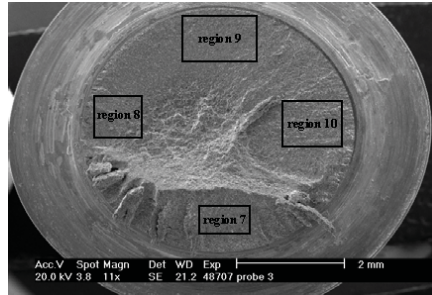


Fig. 6, Fracture surface of tested specimen. Rectangular regions chosen for the fractographical analysis are specified and numbered. The remote mode II acts on the crack front located within the regions 7 and 9, while the remote mode III is present within regions 8 and 10.

The crack path was studied by means of the fracture surface reconstruction of the rectangular regions selected at “top”, “bottom”, “left” and “right” sites, Fig. 7 and Fig. 8. Surface topography was measured by the optical profilometer MicroProf FRT, which uses the chromatic aberration method for determination of the surface height coordinate. An example of the fracture surface reconstruction for mode II (regions 5 and 7) is given as Fig. 7 and surface reconstruction for mode III (regions 4 and 8) is given as Fig. 8.

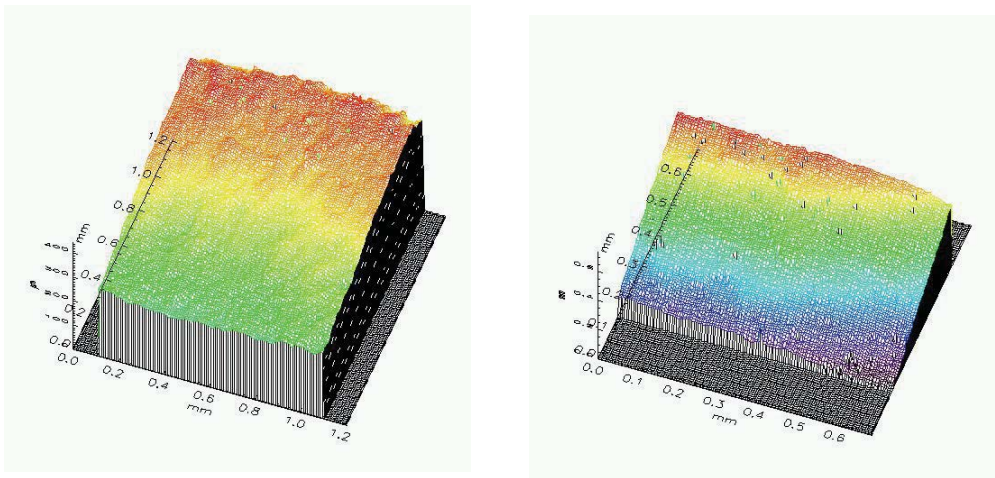


Fig. 7, An example of fracture surface generated by remote mode II: Region 5 (left image) and region 7 (right image).

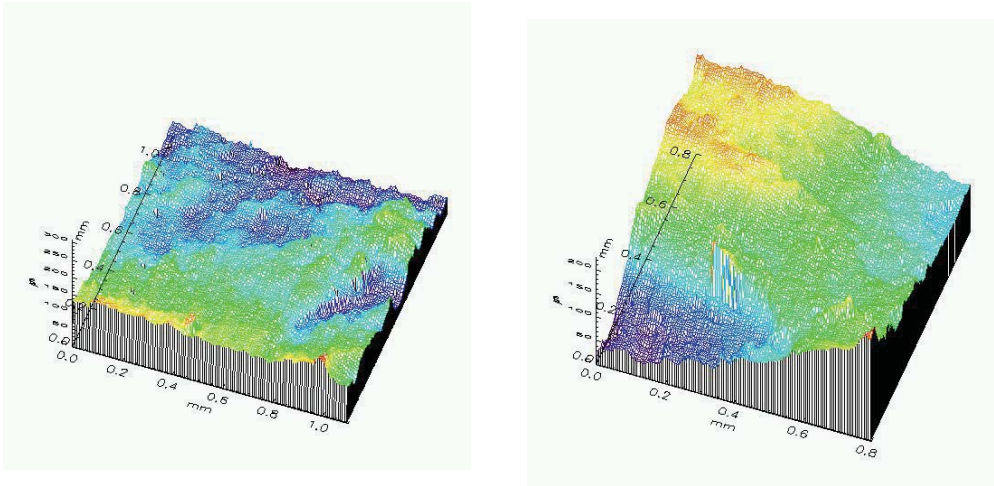


Fig. 8, An example of fracture surface generated by remote mode III: Region 4 (left image) and region 8 (right image).

In the next step, the sets of profiles in both horizontal  $x$ - and  $y$ - axes were extracted from a raw 3D data of each analyzed region and the correlation length,  $\beta$ , which gives the evidence of the crack path “coherence”, was assessed as a quantifying parameter for all profiles. The parameter  $\beta$  was calculated as the shift distance for which the value of the autocorrelation function drops to the 1/10 fraction of its original value,  $R(0)$ . The autocorrelation function is defined as

$$R(p) = \frac{1}{(N-p)} \sum_{k=1}^{N-p} (z_k - \langle z \rangle)(z_{k+p} - \langle z \rangle), \quad (1)$$

where  $N$  is the number of profile data points,  $z$  is the height coordinate,  $\langle z \rangle$  is the mean height and  $p$  is the shift distance [4].

## Results and discussion

Careful study of the surface topography of all analysed regions was carried out by using the software application Mark III, which is supplied with the profilometer MicroProf FRT. It was noted that all the fatigue crack paths exhibited a global deflections from the shear plane within almost all regions, and, therefore, a local mixed mode loading (either modes I+II, I+III, or I+II+III) was experienced by the crack during its propagation. More importantly, qualitatively entirely different topography was observed within the “top” and “bottom” sites and the “left” and “right” sites, see Fig. 7 and Fig. 8. It is obvious, that while in the first case (remote mode II regions) the crack advances in a more or less steady uniform planar manner, a rather complicated propagation of a relatively torturous crack front is observed in the latter case (remote mode III regions).

In order to quantify these differences, the correlation length,  $\beta$ , was used as a conclusive roughness descriptor. The results expressed in terms of the mean values, where the averaging was made over  $x$ - and  $y$ - profile sets separately, and the respective standard deviations are collected in Table 1. Entries belonging to profile sets representing the crack front at subsequent positions are shown in bold. As can be seen from Table 1, distinctive differences of  $\beta$ -values are observed for

profiles parallel with the growing crack front. On the other hand, nearly equal  $\beta$ -values are obtained in the case of profiles perpendicular to the crack growth. This is in accordance with models predicting different growth micromechanisms of mode II and mode III [1,3].

Table 1: The correlation length,  $\beta$ .

Mode	Profiles	$\beta$
II	x	<b>152 ± 34</b>
	y	111 ± 64
III	x	108 ± 12
	y	<b>85 ± 32</b>

## Conclusion

In the paper, a prototype experiment that allows simultaneous mode II and mode III crack propagation in a single specimen was described and first achieved results were discussed. A deflection of the fatigue crack path from the loading shear plane into the plane of opening mode I was found within almost all analysed regions. It is concluded that, based on the 3D observation and the roughness analysis, the crack propagation mechanism is distinctively different within remote modes II and III regions.

## Acknowledgement

The authors acknowledge the support provided by Czech Science Foundation (project 106/08/P366) and the Ministry of Education, Youth and Sports of the Czech Republic (project MSM 0021630518 and 2E08017).

## References

- [1] J. Pokluda, R. Pippan, *Can a pure mode III fatigue loading contribute to crack propagation in metallic materials?* Fat. Fract. Engng. Mater. Struct. Vol. 28 (2005) p. 179.
- [2] J. Pokluda, G. Trattnig, C. Martinschitz, R. Pippan, *Straightforward Comparison of Fatigue Crack Growth under Modes II and III.* Int. J. Fat. Vol. 30 (2008), p. 1498.
- [3] J. Pokluda, K. Slámečka, R. Pippan, O. Kolednik, *Fatigue crack growth in metals under pure mode III: reality or fiction?* In: A. Carpinteri, L.P. Pook: Proc. Fatigue Crack Paths (FCP 2003), Parma 2003, p. 92.
- [4] E.S. Gadelmawla, M.M. Koura, T.M.A. Maksoud, I.M. Elewa, H.H. Soliman, *Roughness parameters.* J. Mat. Proc. Tech. Vol. 123 (2002) p. 133.